
Mechanical Fatigue of Titanium Dental Implants after Implantoplasty: Effect of Material Removal and Finite Element Simulations

[Esteban Padullés-Roig](#) , Pablo Sevilla , [Eugenio Velasco-Ortega](#) , [Miguel Cerrolaza](#) , [Darcio Fonseca](#) , [Jeanne Parache](#) , [Conrado Aparicio](#) , [Javier Gil](#) *

Posted Date: 6 March 2026

doi: 10.20944/preprints202603.0553.v1

Keywords: implantoplasty; dental implants; peri-implantitis; fatigue; fracture; finite element simulation



Preprints.org is a free multidisciplinary platform providing preprint service that is dedicated to making early versions of research outputs permanently available and citable. Preprints posted at Preprints.org appear in Web of Science, Crossref, Google Scholar, Scilit, Europe PMC.

Copyright: This open access article is published under a [Creative Commons CC BY 4.0 license](#), which permit the free download, distribution, and reuse, provided that the author and preprint are cited in any reuse.

Disclaimer/Publisher's Note: The statements, opinions, and data contained in all publications are solely those of the individual author(s) and contributor(s) and not of MDPI and/or the editor(s). MDPI and/or the editor(s) disclaim responsibility for any injury to people or property resulting from any ideas, methods, instructions, or products referred to in the content.

Article

Mechanical Fatigue of Titanium Dental Implants after Implantoplasty: Effect of Material Removal and Finite Element Simulations

Esteban Padullés-Roig¹, Pablo Sevilla⁵, Eugenio Velasco-Ortega³, Miguel Cerrolaza⁴, Darcio Fonseca⁵, Jeanne Parache⁵, Conrado Aparicio^{5,6} and Javier Gil^{5,*}

¹ Faculty of Dentistry. Universidad Internacional de Catalunya, Josep Trueta s/n, Sant Cugat del Vallés, 08195 Barcelona, Spain

² Mechanics Dept. Escuela Universitaria Salesiana de Sarria. Pg. Sant Joan Bosco, 74, 74, 08017 Barcelona, Spain

³ Department of Stomatology, Faculty of Dentistry, University of Seville, c/Avicena s/n, 41009 Sevilla, Spain

⁴ School of Engineering, Science & Technology, Valencian International University. Calle Pintor Sorolla, 21, 46002 Valencia, Spain

⁵ Bioinspired Oral Biomaterials and Interfaces, Department Ciencia e Ingeniería de Materiales, Escola Enginyeria Barcelona Est. Universitat Politècnica de Catalunya. Av, Eduard Maristany 16, 08019 Barcelona, Spain

⁶ ICREA. Institució Catalana de Recerca i Estudis Avançats. Generalitat de Catalunya. 08010-Barcelona. Spain

* Correspondence: javier.gil.mur@upc.edu

Abstract

The increasing prevalence of peri-implantitis has led to a growing clinical use of implantoplasty, a procedure involving intraoral machining of the dental implant surface to remove biofilm. The absence of standardized clinical protocols may contribute to premature fatigue failure of dental implants. The present study aimed to determine the influence of machining depth on the cyclic mechanical behavior of dental implants. A total of 250 commercially pure Grade 3 titanium dental implants were distributed into four groups according to machining depth: untreated (original), 0.2 mm, 0.4 mm, and 0.6 mm wall reduction. The implant system featured an internal connection with a thread height of 0.4 mm. Finite element analysis was performed for each machining depth to evaluate Von Mises stress distribution and to simulate fatigue behavior. The numerical models were validated through experimental fatigue testing using a servohydraulic MTS Bionix testing machine under ISO 14801:2016 standard conditions. Fractographic analysis was conducted by scanning electron microscopy. The results revealed that maximum Von Mises stresses were concentrated at the junction between the implant thread and the implant body. The fatigue limit of the untreated implants was approximately 400 N. Implants subjected to 0.4 mm machining exhibited a fatigue limit of 350 N, whereas lower fatigue limits were observed for 0.2 mm (290 N) and 0.6 mm (180 N) reductions. These findings demonstrate the significant mechanical effect of thread removal. At higher applied loads, fracture occurred in the coronal region of the implant, whereas at lower loads failure shifted to the implant–abutment connection. Finite element predictions showed high agreement with experimental results. The findings highlight a clinically relevant criterion: implantoplasty depth should not exceed the original thread height, as excessive wall reduction markedly compromises fatigue resistance and long-term mechanical reliability.

Keywords: implantoplasty; dental implants; peri-implantitis; fatigue; fracture; finite element simulation

1. Introduction

Peri-implantitis is caused by an inflammatory process triggered by bacterial colonization around the dental implant with the formation of biofilms [1-2]. The consequent persistent inflammation results in bone loss, which ultimately causes the loss of both mechanical and biological fixation of the dental implant [3-5]. Several scientific dental societies have reported that approximately 24% of dental implants develop peri-implantitis within the first 10 years of function [6-7]. In order to reduce these high prevalence rates, preventive strategies have been emphasized, particularly oral hygiene measures and recommendations to avoid smoking and alcohol consumption [8-9]. However, periimplant diseases are also influenced by the patient's genetic susceptibility [10].

The main problem associated with peri-implantitis is bone loss and the difficulty of eliminating biofilms adhering to the implant surface. In principle, the standard approach when removal of the infected dental implant is necessary, would involve disinfection of the surrounding tissues, placement of a calcium phosphate-based biomaterial to induce bone regeneration, and subsequent placement of a new dental implant once regeneration has occurred [11-12]. In many cases, surgery becomes more complex, as placement of a new implant may require extraction of adjacent teeth due to anatomical limitations [13]. This surgical complexity has led to the development of an alternative surgical approach that proposes an aggressive mechanical biofilm removal technique known as implantoplasty. This technique involves mechanical modification of the implant surface intraorally using clinical rotary instruments, particularly highly abrasive burs such as diamond or tungsten carbide burs [14-16]. Subsequently, the machined surface is thoroughly cleaned using disinfecting agents such as hydrogen peroxide, sodium hypochlorite, among others [17]. (Figure 1)



Figure 1. A. Dental implant presenting inflammation in the soft tissues due to peri-implantitis. B. Bone loss caused by the presence of biofilms. C. Dental implant that has undergone mechanization for the removal of biofilms. The loss of roughness and fillets of the dental implant can be seen. The presence of titanium particle debris resulting from mechanization can also be observed.

Implantoplasty is associated with several adverse effects, including loss of surface roughness that promotes osseointegration, reduced corrosion resistance, deterioration of static and cyclic mechanical properties, and the release of particles ranging from nanometric to millimetric sizes. These particles have been shown to exert *in vitro* cytotoxic effects, particularly by particles from dental implants manufactured with the Ti6Al4V alloy [18]. Particle size is a critical factor, as nanoparticles are not recognized by the immune system and their effects on the human body remain unknown [19]. Larger particles, however, may be phagocytosed by macrophages or encapsulated by soft tissue [20]. Kotsakis et al. [21] simulated anaerobic inflammatory conditions in the oral cavity and observed oxygen depletion in the environment, leading to the death of aerobic cells, but not anaerobic cells, which are the most pathogenic. Oxygen depletion causes reduction of the titanium oxide layer of the implant to pure titanium, thereby the passive layer that protects the implant surface might be compromised. When inflammation subsides, oxygen levels in the area recover, reinducing oxidation of pure titanium; however, this oxidation does not result in stoichiometric titanium dioxide but rather in non-stoichiometric mixed oxides that are not cytocompatible. Another major concern is the loss of mechanical properties of dental implants due to machining, as a significant reduction in implant cross-section occurs [22]. This aspect has been poorly studied, particularly with regard to mechanical behavior under cyclic loading.

As described above, implantoplasty is a procedure associated with numerous drawbacks; however, it is currently widely used due to its effectiveness in infection control and its ability to avoid lengthy procedures for the patient, as well as the high cost associated with implant removal, tissue

disinfection, regeneration, and placement of a new dental implant. Various methods have been proposed to avoid titanium machining during implantoplasty, such as electrolysis using the dental implant itself as an electrode, generating hydrogen gas bubbles that remove the biofilm [23]. Fonseca et al. [24] demonstrated the effectiveness of this approach in biofilm removal without altering the titanium properties of the dental implant. Other methods, still under experimental development, include pressurized water jet treatments [25]. Antibiotic therapies and aggressive chemical agents have been discarded, as pharmaceuticals are ineffective in eliminating biofilms and promote antibiotic resistance, while aggressive chemical agents may induce tissue necrosis and acid attack on titanium, increasing surface roughness and thereby favoring subsequent bacterial recolonization of the implantoplasty-treated surface or limiting re-osseointegration of the affected implant [25]. Similarly, ozone treatments do not eliminate biofilms and may cause necrosis of oral soft tissues when applied for prolonged periods [26-27].

The objective of this study is to investigate the influence of implant cross-section reduction due to machining on cyclic mechanical behavior through finite element simulation and validation by mechanical fatigue testing. These results may assist clinicians in determining a safe level of cross-section reduction that prevents fatigue fracture of dental implants in service. The null hypothesis is that cross-section reduction has no influence on fatigue behavior.

2. Materials and Methods

A total of 250 dental implants of 4 mm in diameter (Vega, Klockner, Escaldes Engordany, Andorra), were studied. The dental implants were manufactured with commercially pure grade 3. The roughness (Sa) of the surface was $0.9 \pm 0.2 \mu\text{m}$. The height of the thread was 0.4mm. In Figure 2 can be observed the dental implants studied and the scheme of the thread.

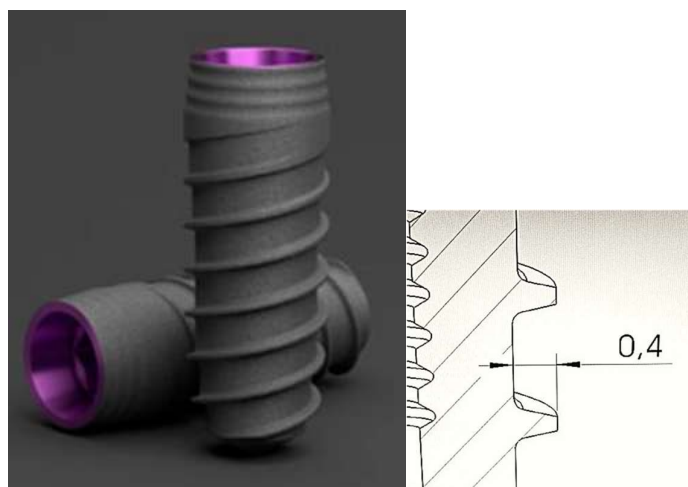


Figure 2. Dental implants studied and scheme of the design of the thread in mm.

Control samples in the as-received condition were characterized, along with four additional sample sets corresponding to distinct implantoplasty procedures. The implantoplasty procedure was carried out by a single dental clinician (E.P.G) to ensure consistency in the treatment protocol and to reduce variability in both surface finish and experimental outcomes. The procedure was carried out using a force-controlled dynamometer to apply consistent pressure between the drill and the titanium surface. The applied force was maintained at a constant load of 10 N using an automatic dynamometric control system, corresponding to the mean force measured by 59 clinicians at the Universitat Internacional de Catalunya's University Dental Clinic. The application of the load lasted 60 s for each disk. The surface of the samples was sequentially modified using a GENTLEsilence LUX 8000B turbine (KaVo Dental GmbH, Biberak, Germany) with continuous irrigation, the surface was sequentially modified with a fine-grained tungsten carbide bur (reference H481. 312.014 KOMET;

GmbH & Co. KG, Lemgo, Germany), and a fine-grained rubber polisher (order no. 9618.314.030 KOMET; GmbH & Co. KG, Lemgo, Germany). (Figure 3)

Implantoplasty was performed at three depths: 0.2, 0.4 (height of the thread) and 0.60 mm. To ensure the thicknesses, all implantoplasties performed were examined under a stereoscopic magnifying glass (Zeiss 400Sb-V, Berlin, Germany) with a resolution of 0.01 mm. Implantoplasties were performed on 200 dental implants, and were selected for each section reduction to ensure the section. The section was measured by stereoscopic magnifier (Olympus, T2400) in all the surfaces and were tested when the differences of the section were ± 0.01 mm.

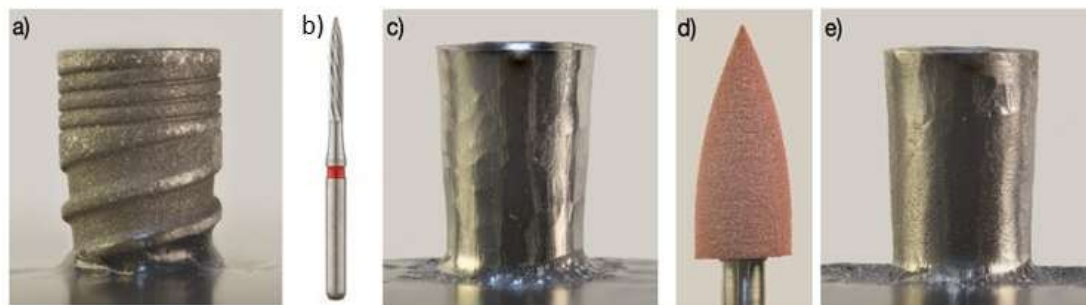


Figure 3. a. Original dental implant. b. Drill of tungsten carbide. c. Implant machined by the drill of WC. d. Drill of particles of rubber to polish the surface. e. Dental implant machined after the implantoplasty.

Finite Element Analysis

A three-dimensional model of the 4 mm Klockner Vega implant was provided by the manufacturer. Modifications were implemented on the model utilizing Altair Inspire 2024 software to accurately simulate the abutment employed in in vitro assays and the implantoplasty procedures.

Model meshing and subsequent static analyses were conducted using HyperMesh software, employing Altair's Optistruct solver. Fatigue analyses were performed utilizing Hyperlife software, also developed by Altair.

The static simulation analysis was performed following the conditions stipulated by the UNE EN-ISO 14801 standard [28]. This standard specifies the application of an external load at a 30° angle, 8mm from the nominal bone level, with the implant embedding plane situated 3mm below this reference level. Figure 4 illustrates the shape of the different implants and the geometric configuration applied during the static analysis.

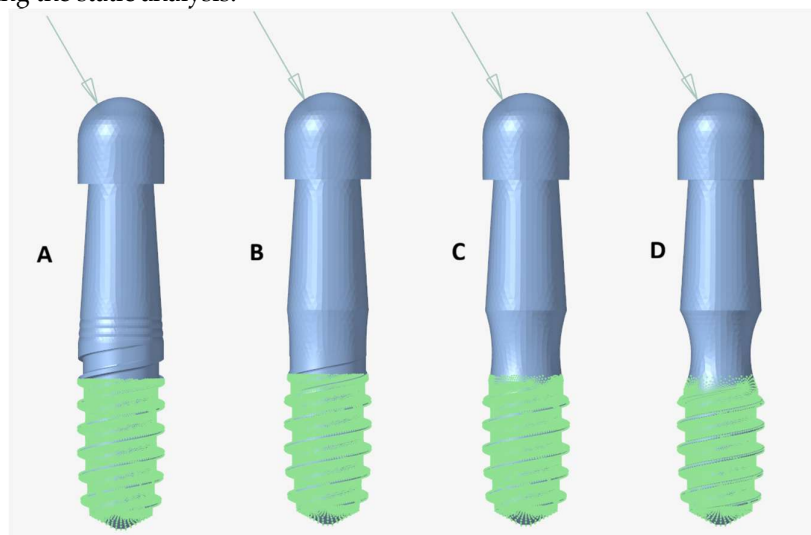


Figure 4. Modelization of the dental implants with different depth of machining. A: Original implant, B: 0.2 mm, C: 0.4 mm, D: 0.6 mm.

The applied load in the static analysis was set to 550 N, corresponding to the maximum load held by the implants during in vitro testing. The implant material was modelled as isotropic bilinear-elastoplastic material, characterized by Young's modulus of 106 GPa, a Poisson's ratio of 0.37, and a yield strength of 550 MPa, based on the manufacturer's specifications. Post-yield behaviour in the plastic region was modelled linearly, with the slope defined by the tangent modulus [29]. The tangent modulus to simulate hardening after the yield point yielding was determined using the Ramberg-Osgood equation [30], by employing a strain hardening exponent of 0.1 and a strength coefficient of 1,000 MPa [31]. This provides yielded a tangent modulus of 2,765 MPa, which was subsequently utilized in the Finite Element Analysis (FEA).

To evaluate the high-cycle fatigue (HCF) behaviour, the material's S-N curve was constructed using relevant material properties and assuming an ultimate tensile strength (UTS) of 680 MPa. An S-N (Stress vs. Number of cycles) analysis was performed based on the von Mises stress results obtained from the static analysis, incorporating the Goodman mean stress correction [32]. The Goodman's criterion was adopted herein as it provides a reliable and conservative estimation for ductile materials, such as the titanium Grade 4 used in this simulation. Unlike the Gerber criterion [32], which may underestimate the effect of mean tensile stresses, or the Soderberg approach [35], which is often excessively restrictive by relying on the yield strength, the Goodman relation effectively balances clinical safety with mechanical reality. This is particularly relevant in dental implantology, where implants are subjected to complex cyclic loading under pre-tension due to screw tightening. By incorporating the Ramberg-Osgood parameters [30] into the plastic behaviour model, the FEA results account for the strain-hardening effects that occur after the yield point, ensuring that the stress distribution used for the S-N analysis reflects the true structural response of the material under maximum functional loads.

Fatigue testing

We carried out fatigue testing in room air and at room temperature using a servo-hydraulic mechanical testing machine (MTS Bionix 370, MTS®, Eden Prairie, USA) equipped with a 15 kN load cell (MTS Load Cell 661.19H-03, MTS®, Eden Prairie, USA). We screwed identical hemispherical abutments to each implant with the torque recommended by the manufacturer (35N·cm). The loading center was located 13 mm above the resin (nominal bone level). According to ISO 14801:2016 [28], we placed the samples in a stainless-steel clamping jaw so that loading had an angle of 30° to the longitudinal axis of the implant (Figure 5).

According to European Standard [28], the general principles for fatigue testing state that "at least two, and preferably three, specimens shall be tested at each of at least four loads. Moreover, "at least three specimens shall be tested, and every specimen shall reach the specified number of cycles with no failures" in order to reach the infinite life range. For all these reasons, a minimum of 9 specimens are necessary (in our study there were 10 samples in the experimental group and 9 in the control group) to meet the requirements of the International Standard.

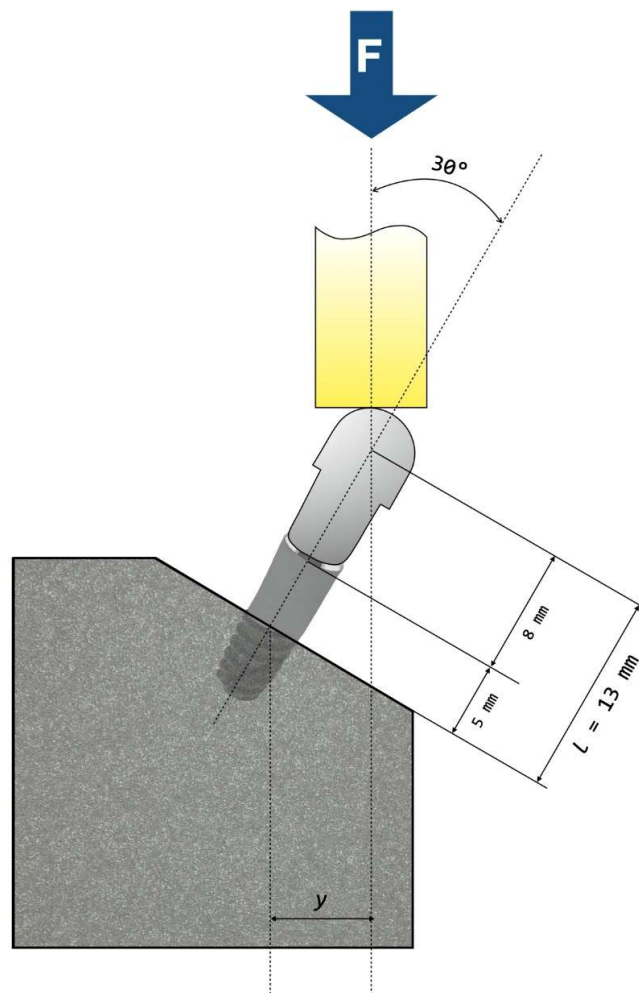


Figure 5. Schematic representation of the test setup according to ISO 14801:2016, except for bone nominal level.

To conclude, it should be noted that while this International Standard simulates de functional loading of an endosseous dental implant under “worst case” conditions, it is not applicable for predicting the in vivo performance of an endosseous dental implant or dental prosthesis, particularly if multiple endosseous dental implants are used for a dental prosthesis.

Each specimen received a maximum of 5,000,000 cycles of a uniaxial load, perpendicular to the tangent of the dome of the hemispherical abutment. Loading range was between a maximal nominal value and 10% of this value ($R = 0.1$). To minimize the vibrations of the testing machine, sinusoidal load frequency was kept at 15 Hz. We used TestStar II® software (MTS®, Eden Prairie, USA) to record data in real time.

In accordance with ISO 14801:2016 [28], tests were carried out applying a minimum of four series of loads, the first of which was equivalent to 80% of the maximum compression force ($F_{\max C}$ and $F_{\max IP}$), which was determined in a previous study to be 735 N and 529 N for the control and IP samples, respectively 21. At each load level, two samples were evaluated, considering 5×10^6 cycles as an infinite life criterion. If any of the samples collapsed before reaching the specified number of cycles, the procedure was started again with two new implants and under a lesser load (20% if $\geq 60\%$ F_{\max} and 10% if $< 60\%$ F_{\max}). When two consecutive samples reached 5×10^6 cycles without failure, an additional test was performed with a third sample. If the latter did not fail (i.e., 3 consecutive samples without apparent failure), this point was considered to be the fatigue limit beyond which the implant could withstand an infinite number of loading cycles. In case the fatigue limit was reached in less than four load series, additional levels (1, 2 or 3) were established by applying a load

5% higher than the previous one. The number of cycles and the state (i.e., intact or failed) of each tested specimen were recorded. Failure was defined as the elastic limit of the material, permanent deformation, loosening of the implant assembly, or fracture of any component. The results of the fatigue tests were displayed in a load versus number of cycles plot (i.e., S-N curve or Wöhler's curve), which represents the number of load cycles of each sample (logarithmic scale) and the corresponding maximal load (linear scale).

Fractography was studied by means of Scanning Electron Microscopy (JEOL 6400) with X-ray microanalysis (Oxford F300).

The number of samples used was obtained by an experimental sample size method. Statistical analysis was performed using MiniTab 17 software (Minitab Inc.). Kruskal-Wallis and Mann Whitney U non-parametric tests were used to compare the different conditions to each other. Statistical differences were considered with $p < 0.005$.

3. Results

The table 1 shows the results of the elements analyzed in the simulation subjected to maximum stress and their corresponding deformation when force is applied under the conditions described in the methodology.

Table 1. Flexural resistance and strain associated for the different models studied with the elements analyzed.

| | Elements analyzed | Von Misses stress (MPa) | Strain |
|-----------------------|-------------------|-------------------------|---------|
| Original | 518759 | 566,2 | 0,02395 |
| Implantoplasty 0,2 mm | 444365 | 571,2 | 0,02999 |
| Implantoplasty 0,4 mm | 373916 | 567,5 | 0,02555 |
| Implantoplasty 0.6 mm | 353345 | 663,7 | 0,13990 |

It can be observed that the implant experiencing the highest stress is the one that has undergone a 0.4 mm implantoplasty, while the implant with the lowest stress is the one that has undergone a 0.2 mm implantoplasty. On the one hand, the intact implant has intermediate stress because, when performing the implantoplasty, the thread in the upper part of the implant is removed, along with the geometry that induces an intensification of stresses in the area subjected to greater flexion. On the other hand, the implant with 0.6 mm has an excessive reduction in cross-section, which causes a significant weakening of the implant. In Figure 6 it can be observed the Von Misses stresses distribution for the different dental implants subjected to stress. The maximum stress is located in the thread-body of the implant.

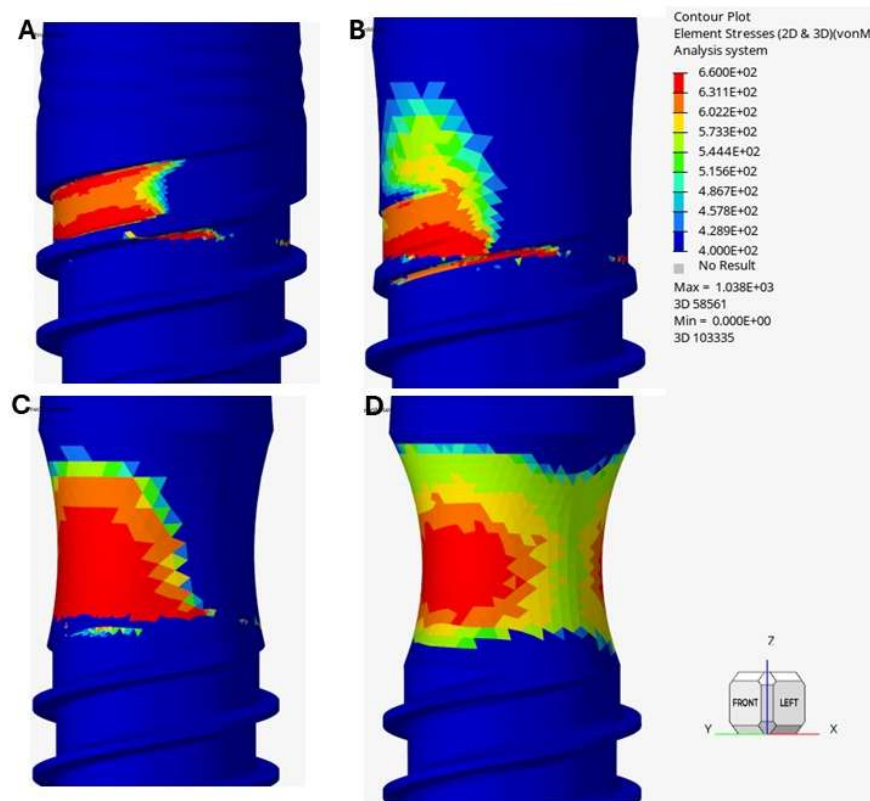


Figure 6. Distribution of Von Mises stress of the four implants subjected to static loading. A. Original implant, B. 0.2 mm implantoplasty, C. 0.4 mm implantoplasty. D. 0.6 mm implantoplasty.

The stress-intensifying effect of the implant thread in the area of maximum stress, located between the flank and the bottom of the thread, can be observed. The maximum stress is distributed over a larger surface area in the treated implants, since the thread has been removed in that area.

The fatigue results can be seen in Figure 7, which shows the S-N curve for the original dental implant, with implantoplasty reduction of 0.2, 0.4, and 0.6 mm of the section. Two clearly differentiated behaviors can be observed: those with low fatigue cycles up to 10.000 cycles approximately and those with high fatigue cycles which were tested until 10.000.000 cycles. It can be seen that the original implants have the highest fatigue life curve, followed by the dental implants subjected to 0.4 mm implantoplasty (i.e., leaving the implant without coils), followed by the dental implants subjected to 0.2 mm implantoplasty. For dental implants with a 0.6 mm reduction, the maximum bending load decreases by almost half and the fatigue curve is much lower than the other three.

Although the ISO standard [28] indicates that the fatigue limit is reached at 5 million cycles, in our case we have reached 10 million because a dental implant must be considered a device that must have mechanical reliability superior to the patient's expected lifespan.

The results show a fatigue limit of approximately 400N for the original dental implant, which means that if the implant is subjected to lower mechanical loads, it will not fracture. For implants with 0.4 mm mechanization in their implantoplasty, this fatigue limit value is 350N; for implants with 0.2 mm implantoplasty, it is 290N; and finally, 180N for implants with the deepest implantoplasty of 0.6 mm.

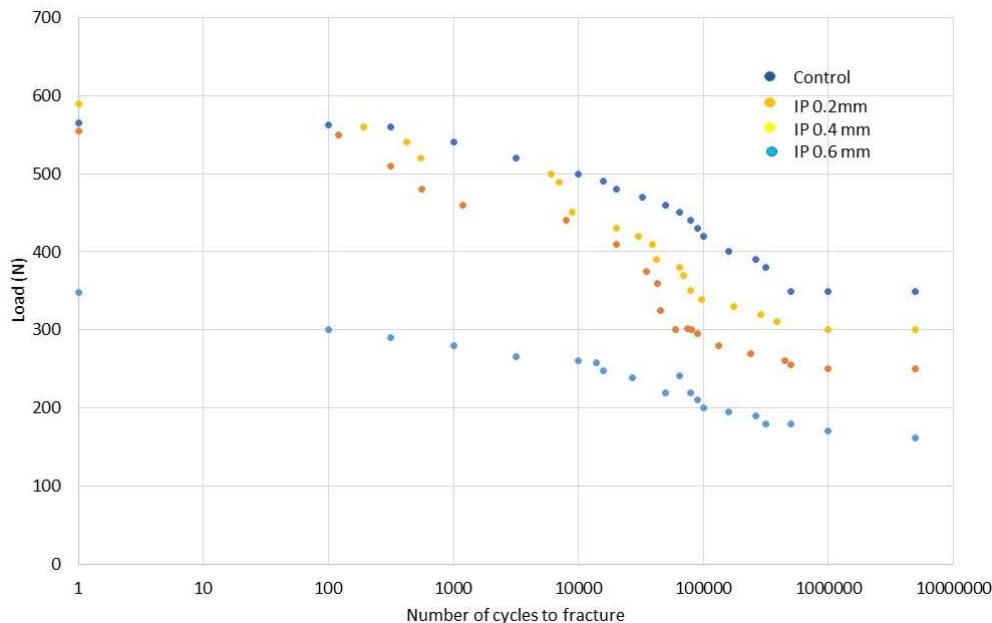


Figure 7. Load-number of cycles to fracture for different dental implants studied.

Fractography studies show that in the first stage of fatigue up to 10,000 cycles, the fracture, corresponding to the highest loads, occurs in the coronal part, as can be seen in Figure 8a, and for a greater number of load cycles, the fracture occurs at the connection between the dental implant and the abutment, as can be seen in Figure 8b. This mode of fracture is appropriate for fatigue behavior as indicated by the ISO standard [28]. The fracture surfaces of the implants subjected to fatigue can be seen in Figure 9. In 9a shows the crack initiation zone, which has a polished surface due to the friction between the fracture faces. The nucleation zones correspond to machining defects on the surface caused by the machining of the implantoplasty. Figure 9b corresponds to the crack propagation zone, where the crack propagation marks can be seen at higher magnifications. Figure 9c corresponds to the final fracture of the implant, which occurred at the connection between the dental implant and the abutment via the Figure 9b corresponds to the crack propagation zone where the crack propagation marks can be seen at higher magnifications. Figure 9c corresponds to the final fracture of the implant, which, as can be seen, has ductile behavior.

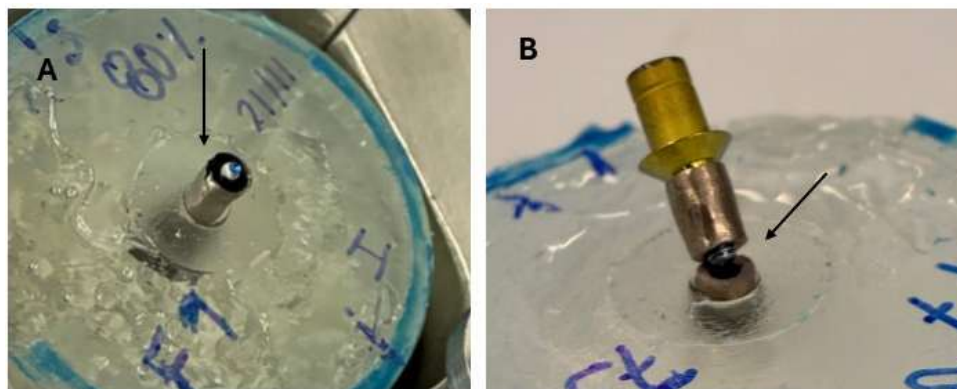


Figure 8. A. Fracture for low number of cycles. B. Fracture for high number of cycles.

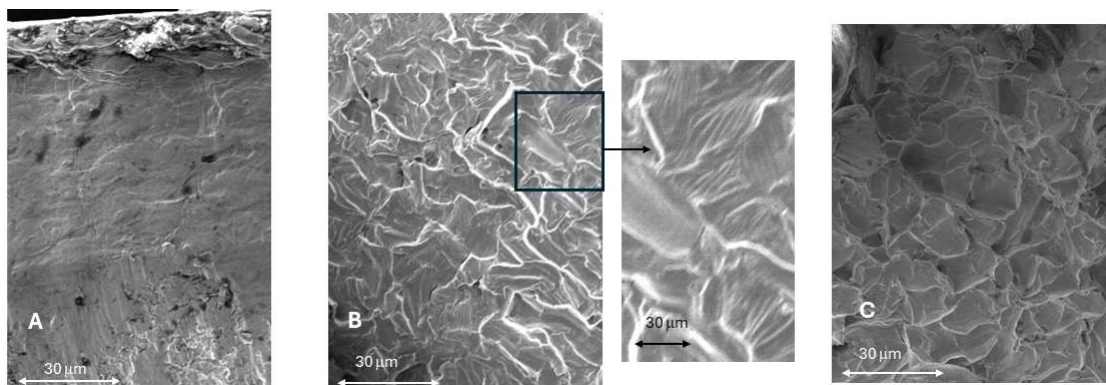


Figure 9. A. Crack nucleation zone. B. Crack propagation. C. Ductile fracture.

When performing the finite element simulation of fatigue behavior, straight lines with two different slopes are obtained for each of the implantoplasties performed. These correspond to low cycle fatigue up to approximately 10,000 cycles and another straight line with a lower slope above this cycle value. It can be seen that the modeling performed is validated by the fatigue tests carried out. This comparison can be observed in Figure 10.

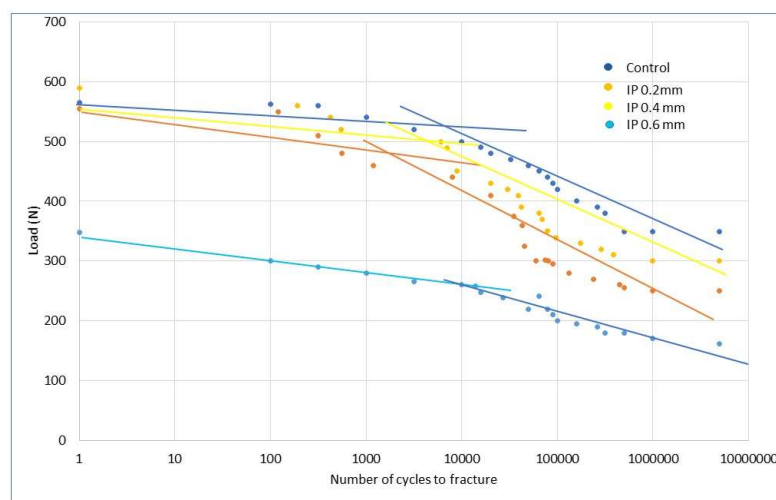


Figure 10. Load-Number of cycles to fracture. The lines are the modelization of the fatigue behavior and the points are the experimental values obtained.

4. Discussion

Implantoplasty is an increasingly employed technique for the removal of biofilm, thereby aiming to halt the progression of bone loss associated with peri-implantitis. Previous studies have demonstrated that this procedure affects the corrosion resistance of the implant surface, as the coexistence of machined and non-machined areas may generate a galvanic couple that promotes corrosion when exposed to the physiological environment [34-35]. Furthermore, implantoplasty produces a smooth surface that is less favorable for fibroblast adhesion, and therefore may hinder the formation of soft tissue capable of contributing to the biological sealing of the implant. Similarly, osteoblast adhesion is not promoted, as it is well established that Sa roughness values between 0.9 and 1.6 μm are optimal for osteoblastic colonization [36]. Consequently, surfaces machined by

implantoplasty present significant limitations for both soft and hard tissue regeneration [36-37]. However, roughness values below 0.088 μm disfavor bacterial colonization of titanium surfaces. [38]. In addition, the release of titanium particles into the surrounding medium may trigger new inflammatory processes and immune responses. The cytotoxicity of titanium particles largely depends on their size and morphology, without considering the still poorly understood biological response to nanoparticles released into the patient's oral cavity [18-19].

The present study aimed to evaluate the effect of controlled implant wall reduction, simulating implantoplasty, on the mechanical properties and in-service cyclic behavior of dental implants. The 30° bending tests revealed a reduction in fracture strength, with a marked decrease when wall reduction exceeded 0.4 mm, corresponding to the height of the implant thread. This finding can be explained by the significant reduction of the load-bearing wall thickness; as the resistant cross-section decreases, the maximum strength is correspondingly and sharply reduced. Fracture was consistently observed at the implant–abutment connection screw interface, which corresponds to the region with the minimum cross-sectional area [39].

Fatigue curve results showed that the original implant (without implantoplasty) exhibited the highest fatigue performance, reaching a fatigue limit above 400 N. Under loads below approximately 400 N, the implant withstood more than 5,000,000 cycles, as required by ISO standards [28], and in our case testing was extended up to 10,000,000 cycles without fracture or plastic deformation. Among the modified implants, the specimen subjected to 0.4 mm implantoplasty—corresponding to complete thread removal—demonstrated the best fatigue performance, with a fatigue limit of approximately 350 N. In contrast, implants subjected to a 0.2 mm reduction exhibited inferior fatigue behavior, with a fatigue limit of approximately 275 N. This behavior can be explained by finite element analysis, which revealed stress concentration at the junction between the thread and the implant body, favoring fatigue crack nucleation. When implantoplasty eliminates the thread entirely (0.4 mm reduction), forming a cylindrical geometry, surface stress concentrations are minimized, resulting in improved fatigue behavior. However, when machining extends beyond the thread into the implant body, the fatigue limit decreases to approximately 180 N. Under such conditions, fatigue fracture may occur between 10,000 and 1,000,000 cycles and, considering physiological masticatory loads, service life would not reach one year.

Fractographic analysis showed that implants subjected to high loads and low cycle numbers fractured at the coronal region. At lower applied loads, fracture occurred at the implant connection where the abutment screw is housed. This fracture mode is accepted by international standards for implant fatigue performance. Fracture occurring in the apical region is not acceptable [40-41]. This consideration is particularly relevant for clinicians managing bruxist patients or individuals with occlusal overload, in whom implantoplasty may adversely affect long-term implant performance [42].

Another relevant factor in implantoplasty is the machining protocol. Initially, diamond or tungsten carbide burs are typically used to remove titanium and biofilm; subsequently, finer burs should be employed to minimize machining defects. Small surface fissures generated during the procedure may act as crack nucleation sites. Therefore, it is essential not to exceed the dimensions of the implant body and to avoid introducing surface defects that could enhance stress concentration and fatigue crack propagation.

To overcome these limitations—namely reduced mechanical reliability, particle release, and decreased corrosion resistance—alternative biofilm removal systems have been investigated. One approach involves electrolytic cleaning, using the implant as a cathode to generate hydrogen bubbles that detach biofilm from the surface. This electrolysis procedure is performed intraorally and is already applied in certain dental clinics. Experimental evidence indicates that this treatment does not impair mechanical properties while effectively cleaning the implant surface. This technique, known as GalvoSurge, is progressively being introduced into clinical practice [24]. Other approaches include high-pressure water jet systems and ozone projection systems aimed at oxidizing and eliminating biofilm-forming bacteria [43]. However, clinical evidence remains inconclusive, and further research

is required to validate the effectiveness of bactericidal treatments that avoid implant machining. It has been developed a novel device, the IMPACT implant planer, designed to machine contaminated implant surfaces intraorally and create a completely smooth surface, thereby promoting peri-implant tissue healing and potential re-osseointegration. This device allows precise control of the machining depth and may therefore help prevent excessive reduction beyond the implant body, particularly beyond the 0.4 mm threshold identified in the present study [44].

Finite element simulations were validated by the experimental results. The modeling accurately predicted stress concentration at the thread–implant body junction near the implant–abutment connection, explaining why a 0.4 mm reduction exhibited better mechanical behavior than a 0.2 mm reduction. Additionally, simulated fatigue curves showed good agreement with experimental fatigue data. Two fatigue regimes were identified: low-cycle fatigue and high-cycle fatigue, with a transition between approximately 1,000 and 10,000 mechanical cycles.

This study has several limitations that should be considered. First, fatigue tests were conducted according to ISO 14801:2016 [28], which does not require testing under physiological conditions at 37°C. It is well established that the physiological environment may reduce fatigue life by accelerating corrosion–fatigue processes in regions of high stored stress [45-48]. Therefore, the reported fatigue life values may vary under in vivo conditions. Another limitation concerns the absence of standardized clinical protocols for implantoplasty. Although the bur sequence used in this study reflects common practice, factors such as applied pressure, duration of machining, and treated area may influence outcomes. Clinically, infected regions do not always involve the entire cylindrical surface exposed to the physiological environment, and surgeons may avoid machining areas where osseointegration is still present. Nevertheless, the present findings provide insight into the influence of implant body wall thickness reduction on fatigue behavior and underscore the importance of avoiding machining depths exceeding the thread height.

5. Conclusions

Experimental results validated the finite element simulations, confirming their ability to predict stress distribution and fatigue behavior. Overall, **implantoplasty depth is critical for long-term implant reliability**; machining should probably not exceed the thread height (**0.4 mm in this study**), and special caution is required in patients with occlusal overload, such as bruxists.

Conflict of Interest Statement. The authors have not any conflict of interest.

Acknowledgements: The authors wish to thank Klockner Medical group the donation of the titanium discs.

Funding: This work was funded by MCIN/AEI/10.13039/501100011033 and FSE+ under award PREVENTITIS-PID2022-137496OB-I00.'

Author Contributions: JG: study conception and design, analysis and interpretation of data, drafting of the manuscript, visualization of the results. MFD: study conception and design, analysis and interpretation of data, PFD; critical revision of the manuscript, administrative support, and study supervision. SO: Investigation, acquisition of different data and interpretation. MC: Investigation; analysis and interpretation of data; visualization of the results; MR: administrative support, technical methods, investigation and study supervision. CA: study conception and design, analysis and interpretation of data, revision. All authors endorsed the final version of the manuscript.

Institutional Review Board Statement: Not applicable.

Informed Consent Statement: Not applicable.

Data Availability Statement: The data that support the findings of this study are available from the corresponding author upon reasonable request.

References

1. Renvert, S.; Roos-Jansåker, A.M.; Claffey, N. Non-surgical treatment of peri-implant mucositis and peri-implantitis: A literature review. *J. Clin. Periodontol.* **2022**, *35* (8 Suppl.), 305–315. <https://doi.org/10.1111/j.1600-051X.2008.01276.x>.
2. Schwarz F, Derks J, Monje A, Wang H-L. Peri-implantitis. *J Clin Periodontol.* 2018;45(S20):S246-S266. doi: <https://doi.org/10.1111/jcpe.12954>
3. Tomasi, C.; Regidor, E.; Ortiz-Vigón, A.; Derks, J. Efficacy of reconstructive surgical therapy at peri-implantitis-related bone defects. A systematic review and meta-analysis. *J. Clin. Periodontol.* 2019, 46 (Suppl. S21), 340–356. <https://doi.org/10.1111/jcpe.13070>.
4. Schwarz, F.; Schmucker, A.; Becker, J. Efficacy of alternative or adjunctive measures to conventional treatment of peri-implant mucositis and peri-implantitis: A systematic review and meta-analysis. *Int. J. Implants Dent.* **2015**, *1*, 22. <https://doi.org/10.1186/s40729-015-0023-1>.
5. Monje, A.; Schwarz, F. Principles of Combined Surgical Therapy for the Management of Peri-Implantitis. *Clin. Adv. Periodontics* 2022, 12, 57–63. <https://doi.org/10.1002/cap.10186>.
6. Diaz P, Gonzalo E, Villagra LJG, Miegimolle B, Suarez MJ. What is the prevalence of periimplantitis? A systematic review and meta-analysis. *BMC Oral Health.* 2022/10/19 2022;22(1):449. doi:10.1186/s12903-022-02493-8
7. Thakkar R. Trends in Dental Implants 2022. American Academy of Implant Dentistry. Accessed January 12, 2025, <https://connect.aaaid-implant.org/blog/trends-in-dentalimplants-2022>.
8. Bhatia AP, Rupamalini SN, Sathi KV, Marella VG, Pendyala SK, Purohit J, Tiwari RV. Impact of the Habit of Alcohol Consumption on the Success of the Implants: A Retrospective Study. *J Pharm Bioallied Sci.* 2024 ;16(Suppl 1):S146-S148. doi: 10.4103/jpbs.jpbs_430_23.
9. Schwarz, F.; Derks, J.; Monje, A.; Wang, H.L. Peri-implantitis. *J. Clin. Periodontol.* **2018**, *45* (Suppl. S20), S246–S266.
10. Silva, D.M.; Castro, F.; Martins, B.; Fraile, J.F.; Fernandes, J.C.H.; Fernandes, G.V.O. The influence of the gingival phenotype on implant survival rate and clinical parameters: A systematic review. *Evid. Based Dent.* **2025**.
11. Fernandes, G.V.d.O.; Martins, B.G.d.S.; Fraile, J.F. Revisiting peri-implant diseases in order to rethink the future of compromised dental implants: Considerations, perspectives, treatment, and prognosis. *Dent. Med. Probl.* **2024**, *61*, 637–640.
12. Mojaver, S.; Fiorellini, J.P.; Sarmiento, H. Advancing peri-implantitis treatment: A scoping review of breakthroughs in implantoplasty and Er:YAG laser therapies. *Clin. Exp. Dent. Res.* **2025**, *11*, e70104.
13. Martins, B.; Fernandes, J.; Martins, A.; Castilho, R.; Fernandes, G. Surgical and Nonsurgical Treatment Protocols for Peri-implantitis: An overview of Systematic Reviews. *Int. J. Oral Maxillofac. Implant.* **2022**, *37*, 660–676.
14. Monje, A.; Pons, R.; Amerio, E.; Wang, H.L.; Nart, J. Resolution of peri-implantitis by means of implantoplasty as adjunct to surgical therapy: A retrospective study. *J. Periodontol.* 2022, 93, 110–122. <https://doi.org/10.1002/JPER.21-0103>.
15. Bertl, K.; Isidor, F.; von Steyern, P.V.; Stavropoulos, A. Does implantoplasty affect the failure strength of narrow and regular diameter implants? A laboratory study. *Clin. Oral Investig.* 2021, 25, 2203–2211. <https://doi.org/10.1007/s00784-020-03534-8>.
16. Toledano-Serrabona, J.; Gil, F.J.; Camps-Font, O.; Valmaseda-Castellón, E.; Gay-Escoda, C.; Sánchez-Garcés, M.Á. Physicochemical and Biological Characterization of Ti6Al4V Particles Obtained by Implantoplasty: An In Vitro Study. Part I. *Materials* 2021, 14, 6507. <https://doi.org/10.3390/ma14216507>.
17. Padulles-Gaspar E, Padulles-Roig E, Cabanes G, Pérez RA, Gil J, Bosch BM. Effects of Hypochlorous Acid and Hydrogen Peroxide Treatment on Bacterial Disinfection Treatments in Implantoplasty Procedures. *Materials (Basel).* 2023;16(8)doi:10.3390/ma16082953
18. Toledano-Serrabona, J.; Bosch, B.M.; Díez-Tercero, L.; Gil, F.J.; Camps-Font, O.; Valmaseda-Castellón, E.; Gay-Escoda, C.; Sánchez-Garcés, M.A. Evaluation of the inflammatory and osteogenic response induced by titanium particles released during implantoplasty of dental implants. *Sci. Rep.* **2022**, *12*, 15790.

19. Barrak, F.N.; Li, S.; Muntane, A.M.; Jones J.R. Particle release from implantoplasty of dental implants and impact on cells. *Int J Implant Dent* 2020, 6, 1–9. doi: 10.1186/s40729-020-00247-1.
20. Wu X, Cai C, Gil J, Jantz E, Al Sakka Y, Padiál-Molina M, Suárez-López Del Amo F. Characteristics of Particles and Debris Released after Implantoplasty: A Comparative Study. *Materials* 2022; 15:602. <https://doi.org/10.3390/ma15020602>.
21. Kotsakis GA, Xie L, Siddiqui DA, Daubert D, Graham DJ, Gil FJ. Dynamic assessment of titanium surface oxides following mechanical damage reveals only partial passivation under inflammatory conditions. *Npj Mater Degrad.* 2024;8(1): 98.doi:10.1038/s41529-024-00514-1
22. Bertl, K.; Isidor, F.; Vult von Steyern, P.; Stavropoulos, A. Does implantoplasty affect the failure strength of narrow and regular diameter implants? A laboratory study. *Clin. Oral Investig.* 2021, 25, 2203–2211.
23. Gianfreda F, Punzo A, Pistilli V, Bollero P, Cervino G, D'Amico C, Cairo F, Cicciù M. Electrolytic Cleaning and Regenerative Therapy of Peri-implantitis in the Esthetic Area: A Case Report. *Eur J Dent.* 2022;16(4):950-956. doi: 10.1055/s-0042-1750773.
24. Fonseca D, Pons R, de Tapia B, Monje A, Nart J, Aparicio C, Gil J. Effect Of Electrolytic Cleaning on Mechanical Properties for Titanium Dental Implants with Surface Contamination. *Int J Oral Maxillofac Implants.* 2025;40(6):725-734. doi: 10.11607/jomi.11082.
25. Kotsakis, G.A.; Lan, C.; Barbosa, J.; Lill, K.; Chen, R.; Rudney, J.; Aparicio, C. Antimicrobial Agents Used in the Treatment of Peri-Implantitis Alter the Physicochemistry and Cytocompatibility of Titanium Surfaces. *J. Periodontol.* 2016, 87, 809–819. <https://doi.org/10.1902/jop.2016.150684>
26. Giok, K.C.; Menon, R.K. The Microbiome of Peri-Implantitis: A Systematic Review of Next-Generation Sequencing Studies. *Antibiotics* 2023, 12, 1610.
27. Herrera, D.; Berglundh, T.; Schwarz, F.; Chapple, I.; Jepsen, S.; Sculean, A.; Kebschull, M.; Papapanou, P.N.; Tonetti, M.S.; Sanz, M. Prevention and treatment of peri-implant diseases—The EFP S3 level clinical practice guideline. *J. Clin. Periodontol.* 2023, 50, 4–76.
28. ISO14801. Dentistry - Implants - Dynamic loading test for endosseous dental implants (ISO 14801:2016) 2016.
29. Callister, W.D.; Rethwisch, D.G. *Materials Science and Engineering: An Introduction*, 10th ed.; Wiley: Hoboken, NJ, USA, 2018.
30. Ramberg, W.; Osgood, W.R. Description of stress-strain curves by three parameters; Technical Note No. 2. 902; National Advisory Committee for Aeronautics: Washington, DC, USA, 1943.
31. Niinomi, M. Mechanical properties of biomedical titanium alloys. *Mater. Sci. Eng. A* 1998, 243, 231–236. [https://doi.org/10.1016/S0921-5093\(97\)00806-X](https://doi.org/10.1016/S0921-5093(97)00806-X).
32. Budynas, R.G.; Nisbett, J.K. Shigley. *Mechanical Engineering Design*, 11th ed.; McGraw-Hill: NY, USA, 2019.
33. Soderberg, C.R. Working stresses. *J. Appl. Mech.* 1935, 57: A106–A108.
34. Aparicio C, Gil FJ, Fonseca C, Barbosa M., Planell JA. Corrosion behaviour of commercially pure titanium shot blasted with different materials and sizes of shot blasted with different materials and sizes of shot particles for dental implant applications". *Biomaterials.* 2003; 24: 263-273.
35. Lozano P, Peña M, Herrero-Climent M, Rios-Santos JV, Rios-Carrasco B, Brizuela A, Gil J. Corrosion Behavior of Titanium Dental Implants with Implantoplasty. *Materials (Basel).* 2022; 19;15(4):1563. doi: 10.3390/ma15041563.
36. Aparicio C, Manero JM, Conde F, Pegueroles M, Planell JA, Vallet-Regí M, Gil FJ. Acceleration of apatite nucleation on microrough bioactive titanium for bone-replacing implants. *J Biomed Mater Res A.* 2007; 1;82(3):521-9. doi: 10.1002/jbm.a.31164.
37. Kunrath, M.F.; Garaicoa-Pazmino, C.; Giraldo-Osorno, P.M.; Mustafa, A.H.; Dahlin, C.; Larsson, L.; Farah Asa'ad, F. Implant surface modifications and their impact on osseointegration and peri-implant diseases through epigenetic changes: A scoping review. *J. Periodontal Res.* 2024, 59, 1095–1114.
38. Rimondini L, Farè S, Brambilla E, Felloni A, Consonni C, Brossa F, Carrassi A. The effect of surface roughness on early in vivo plaque colonization on titanium. *J Periodontol.* 1997; 68(6):556-62. doi: 10.1902/jop.1997.68.6.556.
39. Gil, F.J.; Planell, J.A. Aplicaciones biomédicas del titanio v sus aleaciones. *Biomecánica* 1993, 1, 34–43.

40. Fonseca D, de Tapia B, Pons R, Aparicio C, Guerra F, Messias A, Gil J. The Effect of Implantoplasty on the Fatigue Behavior and Corrosion Resistance in Titanium Dental Implants. *Materials (Basel)*. 2024 Jun 15;17(12):2944. doi: 10.3390/ma17122944.
41. Toledano-Serrabona, J.; Sánchez-Garcés, M.A.; Gay-Escoda, C.; Valmaseda-Castellon, E.; Camps-Font, O.; Verdeguer, P.; Molmeneu, M.; Gil, F.J. Mechanical properties and corrosión behavior of Ti6Al4V particles obtained by Implatoplasty. An in vivo study. Part. II. *Materials* 2021, 14, 6519.
42. Komiyama O, Lobbezoo F, De Laat A, Iida T, Kitagawa T, Murakami H, Kato T, Kawara M. Clinical management of implant prostheses in patients with bruxism. *Int J Biomater*. 2012;2012:369063. doi: 10.1155/2012/369063.
43. Ambrosio D, Caggiano F, Acerra M, Pisano A, Giordano F. Is Ozone a Valid Adjuvant Therapy for Periodontitis and Peri-Implantitis? A Systematic Review. *J Pers Med*. 2023 Apr 8;13(4):646. doi: 10.3390/jpm13040646. 42
44. Fernandes, G.V.O.; Martins, B.G.d.S.; Fernandes, J.C.H.; Gabet, Y.; Vizanski, A. The Novel iMPACT Tool and Quadrant Protocol for Peri-Implantitis: Surface Refinement and Re-Osseointegration Validated by SEM/EDS and Long-Term Clinical Case Reports. *Medicina* 2025, 61, 1094. <https://doi.org/10.3390/medicina61061094>
45. Eliaz N. Corrosion of Metallic Biomaterials: A Review. *Materials (Basel)*. 2019; 28;12(3):407. doi: 10.3390/ma12030407.
46. Asri RIM, Harun WSW, Samykano M, Lah NAC, Ghani SAC, Tarlochan F, Raza MR. Corrosion and surface modification on biocompatible metals: A review. *Mater Sci Eng C Mater Biol Appl*. 2017; 1;77:1261-1274. doi: 10.1016/j.msec.2017.04.102.

Disclaimer/Publisher's Note: The statements, opinions and data contained in all publications are solely those of the individual author(s) and contributor(s) and not of MDPI and/or the editor(s). MDPI and/or the editor(s) disclaim responsibility for any injury to people or property resulting from any ideas, methods, instructions or products referred to in the content.